Extended Abstracts of the 2014 International Conference on Solid State Devices and Materials, Tsukuba, 2014, pp34-35

Properties of ultrathin body condensation GOI films thinned by additional thermal oxidation

WuKang Kim[1, 2], Mitsuru Takenka[1, 2], and Shinichi Takagi[1, 2]
[1]The University of Tokyo, 7-3-1 Hongo, Bunkyo-ku, Tokyo, 113-8656, Japan, [2]JST-CREST
Phone & FAX: +81-3-5841-6733, Email: wukangkim@mosfet.t.u-tokyo.ac.jp

Abstract **We report the physical and electrical characteristics of ultra-thin GOI (Ge-On-Insulator) thinned by additional oxidation after the Ge condensation process. This process can realize GOI thickness down to around 6 nm. Increase in additional oxidation time leads to continuous change in strain from compressive to tensile one and increase in residual hole concentration of GOI, which can be explained by defect generation. We demonstrate the operation of 9.7-nm-thick GOI pMOSFETs. The effective mobility decreases with a decrease in the GOI thickness.**

1. Introduction Among a variety of the high mobility MOS channel materials [1], Ge is regarded as one of the most promising materials because of its characteristics of both high hole and electron mobility and easy introduction into the Si platform. In addition, a UTB (ultra-thin body) GOI (Ge-On Insulator) structure is also crucial for suppressing short channel effects in scaled devices. Here, it is important to understand the physical and electrical characteristics of GOI layers with the thickness of around 10 nm or less, judging from the applied technology nodes. However, there are quite few studies on these characteristics, because the realization of such thin GOI films is not easy. One of the most promising techniques to fabricate such UTB GOIs is the Ge condensation method [2, 3]. In this study, we fabricate GOI layers with the thickness down to 6 nm by additional oxidation of GOI formed by Ge condensation and successfully demonstrate the 9.7-nm-thick GOI pMOSFET operation. We analyze the physical and electrical characteristics of the GOI layers and have examined the GOI thickness dependence.

2. Experimental Fig. 1 shows the process flow of the present UTB GOI layers by the Ge condensation and successive additional oxidation process for thinning the GOI body. The Ge condensation process was performed with changing the oxidation temperatures from 1100, 1050, 1000, 950 to 900 ^{o}C. Here, the SiGe-OI wafers were annealed in dry N_2 at 1050 ^{o}C, 1000 ^{o}C and 950 ^{o}C after each oxidation step during this condensation process. The thickness of the fabricated GOI was 14.3 nm. After that, additional oxidation was carried out at 900 ^{o}C for 10, 30, 50, 70, and 90 minutes without removing 200 nm SiO_2 layers capping GOI, in order to form thinner GOI layers. As a result, we have successfully achieved the GOI thickness of 10 nm or less. A TEM photograph (Fig. 2) shows that the thickness of the GOI layer oxidized for 50 minutes is 9.7 nm. The thickness of the GOI layers oxidized for 10, 30, 50, 70 and 90 minutes is estimated to be around 13.2, 11.4, 9.7, 8.0, and 6.5 nm, respectively (Fig. 3). Raman spectroscopy was used for evaluating the GOI films. Also, the Hall measurement was used to measure the hole concentration of the GOI layers. Here, the Hall devices and MOSFETs were fabricated by depositing Ni and Al for the S/D contact and the back contact, respectively. The Hall devices and MOSFETs operated under the back gate configuration.

3. Experimental Results Fig. 4 shows the Raman spectra for the thinned GOIs. While the GOI layer with no additional oxidation has compressive strain in most of the areas, the GOI layers after the additional oxidation have tensile strain. It is found in Fig. 5 that, as the oxidation time becomes longer, tensile strain is higher. Note that the most of the area of the GOI with no additional oxidation has compressive strain, though the limited areas with tensile strain are locally observed. The compressive strain in the GOI films with no additional oxidation is attributed to the remaining strain due to the lattice mismatch between Ge and Si [2]. It is known, on the other hand, that the higher coefficient of thermal expansion of Ge than Si or SiO_2 [4] leads to tensile strain in Ge films after high temperature process. Since the total strain could combine these two effects, the change in strain from compressive to tensile during the additional oxidation one suggests the continuous relaxation of remaining compressive strain due to the larger lattice constant of Ge during additional oxidation after condensation. Actually, we have found the increase in the full width at half maximum (FWHM) of the Raman spectra with longer additional oxidation time, as shown in Fig. 6. These findings indicate that additional oxidation causes the relaxation of remaining compressive strain in GOI by introducing any defects or dislocation in GOI [5], which might lead to the increase in FWHM of the Raman spectra.

We have measured hole concentration of the GOI layers after additional oxidation by Hall measurement. Fig. 7 shows the hole concentration of the GOI layers as a function of the GOI thickness. The hole concentration of the initial GOI layer, fabricated by the optimized Ge condensation process [6], is as low as 2.2×10^{17} cm^{-3}. However, the hole concentration increases with additional oxidation. The concentration of 13.2, 11.4 and 9.7- nm thick GOI, after additional oxidation for 10, 30 and 50 minutes, amounts to 4.8 x 10^{17}, 2.8 x 10^{18} and 7.9 x 10^{18} cm^{-3}, respectively. Note that the electric characterization of the 8.0- and 6.5-nm-thick GOI devices was unsuccessful because of the large leakage current through buried oxide. This increase in the hole concentration after the additional oxidation can also be explained by the generation of defects or dislocations, probably due to the relaxation of remaining compressive strain, which is evident in the results of Fig. 6.

Fig. 8 shows the I_d-V_g characteristics for GOI pMOSFETs with different GOI thickness. The MOSFETs operate under the accumulation mode. V_{th} of the I_d-V_g curves is shifted toward positive direction with thinning the GOI thickness, which is attributed to the increase in the hole concentration. Fig. 9 shows the effective hole mobility of GOI pMOSFETs. The mobility is degraded with thinning the GOI thickness. In particular, larger degradation in a low N_s region can be explained by the increase in Coulomb scattering due to higher acceptor concentration in the thinner body. On the other hand, the mobility in the 9.7-nm-thick GOI becomes lower in whole N_s region. Since this effective mobility is in good agreement with the measured Hall mobility, the mobility degradation in in the 9.7-nm-thick GOI is attributable to the degradation of the crystal quality due to the generated defects.

4. *Conclusion* In this study, we have thinned the GOI layers down to around 6 nm by additional oxidation after the Ge condensation process. The change in strain from compressive to tensile strain and the increase in hole concentration have been found with thinning GOI layers. We have also

demonstrated operation of 9.7-nm-thick GOI pMOSFETs.
Acknowledgements This work was partly supported by a Grant-in-Aid for Scientific Research on Priority Area (No. 26249038) from the Ministry of Education, Culture, Sports, Science, and Technology in Japan.

References [1] S. Takagi *et al.*, SSE **51.** 526 (2007) [2] S. Nakaharai *et al.*, APL **83**, 3561 (2003) [3] K. Ikeda *et al.*, SSDM, 32 (2008) [4] G. A. Slack et al., JAP, **46**, 89 (1975) [5] S. Nakaharai et al., Semicond. Sci. Technol. **22** (2007) S103 [6] W.-K. Kim et al., SSDM, 774 (2013)

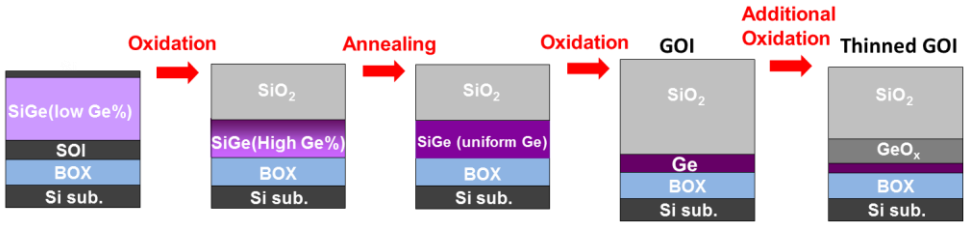

Fig. 1 Process flow of GOI by Ge condensation and additional oxidation

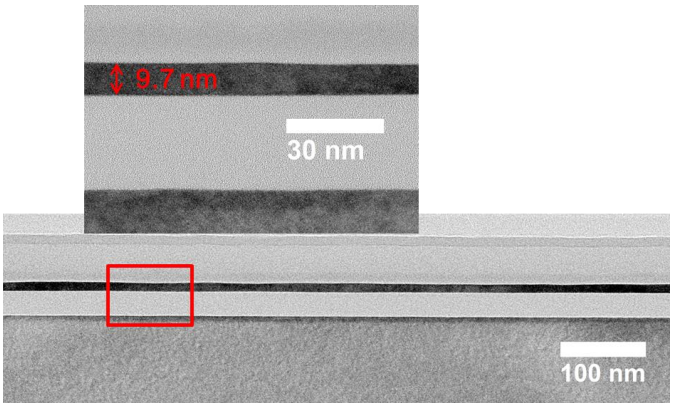

Fig. 2 TEM image of a GOI layer

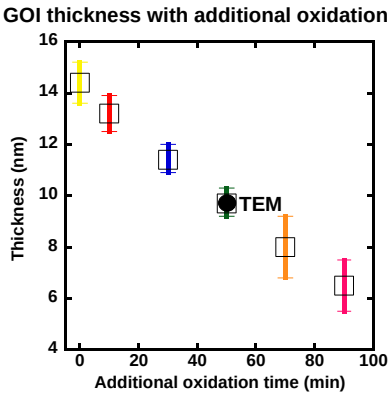

Fig. 3 GOI thickness as a function of additional oxidation time

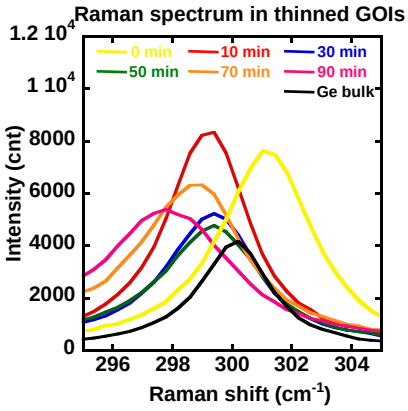

Fig. 4 Raman spectrum in thinned GOIs

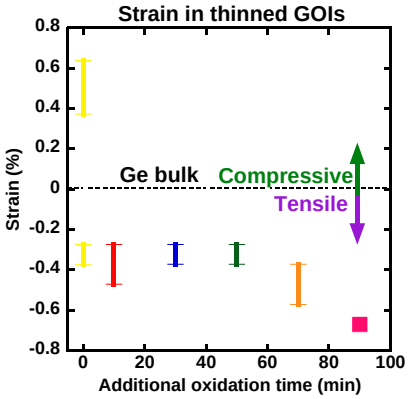

Fig. 5 Strain of thinned GOIs

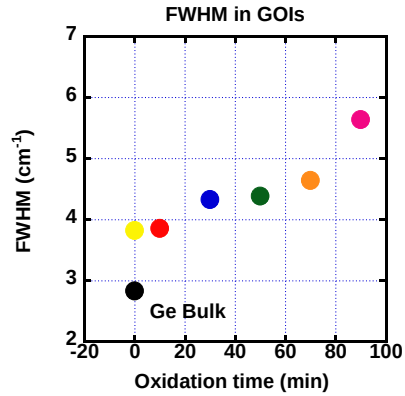

Fig. 6 FWHM in thinned GOIs

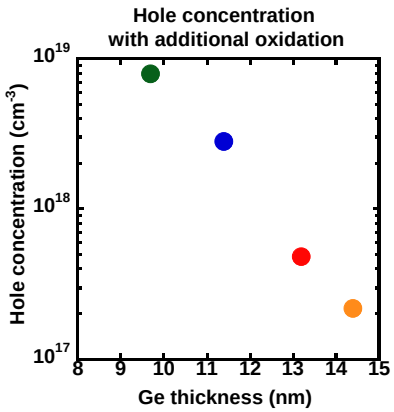

Fig. 7 Hole concentration of thinned GOI layers

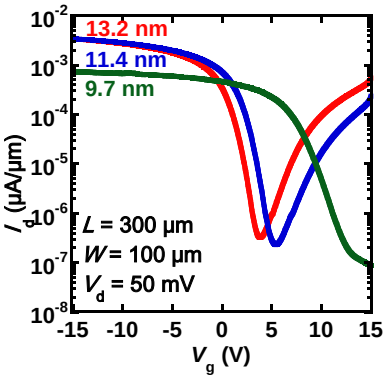

Fig. 8 I_d-V_g characteristics of UTB GOI pMOSFETs

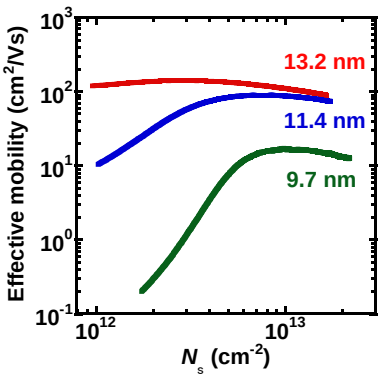

Fig. 9 Effective mobility of UTB GOI pMOSFETs